

Supporting Information:

5 **Single-Molecule Imaging of DNA Duplex Immobilized on Surfaces with Scanning Tunneling Microscope**

Takahito Ohshiro, Mizuo Maeda

Bioengineering Laboratory, RIKEN (The Institute of Physical and Chemical Research

Supporting Experimental Section.

10 **Probe DNA immobilization and target DNA hybridization.**

Synthesized probe DNA and target DNA were purchased (Tsukuba Oligo, Operon Japan). For immobilization of thiolate probe DNA on gold substrates, we prepared 1 μ M probe DNA, 12.5 mM MgCl₂ and 10 mM Tris buffer solution (pH 7.3). After gold substrates (Sigma-Aldrich, Tokyo, Japan) were annealed by hydrogen flame, they were exposed to the probe DNA solution for 1 day. After DNA
15 probe immobilization, the substrates were immersed in a solution containing 1 μ M target DNA, 12.5 mM MgCl₂, and 10 mM Tris buffer (pH 7.3). The substrates were rinsed with fresh buffer solution to remove target DNA non-specifically bound on the substrates, and then used for STM measurements. After annealing the gold substrate using a hydrogen flame, we observed a STM image of the bare gold substrate in 10 mM phosphate buffer (pH 7.3) containing 50 mM NaCl. Figure S4 d shows a typical
20 STM image of a gold substrate. The triangular shaped area consisted of a gold terrace which was higher than the other portion by 0.24 nm (Figure S4 e), i.e., comprised a monatomic step of gold, which is similar to previous reports. This confirmed that the prepared substrates comprised clean Au (111) substrates. This confirmed that the prepared substrates are clean Au (111) substrate. The immobilization of probe DNA and the hybridization of target DNA were also confirmed by SPR and electrochemical
25 measurements (**ref.S1, and S2**) in the following section (**Supporting Information Results**).

***In situ* STM tip preparation**

STM tips were prepared from gold wire (0.25 mm diameter; Nilaco, Tokyo, Japan) by electrochemical etching in 3 M NaCl with 10 V AC and washed in an ultrasonic bath or cleaned in piranha solution. The tips were then washed in an ultrasonic bath or cleaned in piranha solution (7:3 concentrated H₂SO₄/30% H₂O₂/70%. *Caution: piranha solution reacts violently with organic compounds and should not be stored in closed containers.*). To keep faradic currents low during *in situ* STM measurements, the tips were coated with polydimethylsiloxane (Silipot 108, Torei Dow Corning, Japan) or Apiezon Wax (Nilaco, Japan). These gold tips were used for *in situ* STM measurements of DNA duplexes. We also used polydimethylsiloxane coated Pt/Ir tips (0.25 mm diameter; Nilaco, Tokyo, Japan) for STM measurements, and obtained the single-molecule images of DNA duplexes as same as the images by using the gold tips.

***In situ* STM measurements for single-stranded or DNA duplexes immobilized on gold substrates**

We used a Nanoscope IIIa (Digital Instruments, USA) for STM measurements. The STM measurements were performed in *in situ* STM mode. Ag/AgCl wire electrode and platinum wires (0.25 mm diameter; Nilaco, Tokyo, Japan) were used for the reference and counter-electrodes, respectively. All measurements were performed in 10 mM phosphate buffer (pH 7.3) containing 50 mM NaCl. To achieve an upright orientation of DNA duplexes, the sample substrate was kept at -300 mV (vs. the Ag/AgCl reference electrode) **before** the STM measurements. DNA duplexes immobilized on substrates were used for the STM measurements. For the STM measurements, the sample substrate was always observed at the substrate potential (E_{sub}) of -200 mV, and the bias voltage (E_{bias}) was +200 mV (sample negative), where E_{bias} is defined as the tip potential (E_{tip}) relative to the substrate potential (E_{sub}) ($E_{bias} = E_{tip} - E_{sub}$). In a previous study, DNA duplexes on substrates were investigated with AFM under an applied potential of -200 mV, which is the same applied potential as that employed in our STM study. The observed thickness of the DNA oriented perpendicular to the substrates was comparable with the

length of the DNA duplexes, suggesting that the DNA duplexes were not distorted (ref. 8). Therefore, we supposed that the DNA duplexes would also be stable and not distorted under this applied potential during the scanning in our study. The tunneling current was in the range of 200-1200 pA. All STM images comprised 512 x 512 pixels, and are shown as raw data.

5

Procedures for electrochemical measurements.

All electrochemical measurements were performed with a BAS 100B electrochemical analyzer. Cyclic voltammetry (CV) was carried out with a conventional three electrode system, consisting of a bare or modified gold working, a platinum flag auxiliary electrode, and a Ag/AgCl/3.0 M NaCl
10 reference electrode (Bioanalytical System Inc.,). All potentials are reported versus Ag/AgCl reference at room temperature. The solution was degassed with argon for at least 30 min prior to data acquisition. Cyclic voltammetry was conducted at a sweep rate of 100 mVs⁻¹ between -400 mV and +600 mV for [FeCN₆]^{-4/-3} redox reaction, and between -600 mV and -200 mV for AQDS redox reaction .

15 Procedures for SPR measurements

The probe DNA immobilized sensor-chip was prepared as same as that used for STM sample preparation. Gold sensor substrate (SIA cell; Biocare) was exposed to a 1 μM solution of thiolated DNA for 120 min, and the cell was then rinsed with phosphate buffer solution, prior to SPR measurements (Biocore T100). For measurements of the binding amount of hybridized target DNA in
20 which a probe DNA film was exposed to a series of concentrations of the target, experiments were performed until steady-state hybridization was reached under flow conditions (10 μL/min for 180 s)). Target DNA concentrations in the range 500 nM were used. A control experiment, using a non-complementary target DNA (random MM) solution, confirmed that non-specific binding was completely absent. The sensor cell of probe DNA immobilized substrate was repeatedly used for various
25 target DNA hybridization sensing. The regeneration of the single-stranded probe film after

hybridization experiments was achieved by denaturation of the surface duplex by rinsing with 1mM NaOH solution. Highly reproducible behavior is observed for the sensor cell generated on different gold substrates provided that the probe density is identical. All solutions were prepared with MillQ water. For immobilization of thiolated DNA, solutions were prepared as 1 μ M thiol in 10m M phosphate buffer. Hybridization solutions were prepared as 1 μ M target in 12.5 mM MgCl₂ containing phosphate buffer (pH 7.6) and 1mM EDTA)

Calculation of the measured values for molecular density ($M_{density}$), the STM tip heights for DNA molecules (h_{DNA}), and molecular diameter of DNA molecules (ϕ_{DNA})

Each value of the molecular density ($M_{density}$), STM tip heights for DNA molecules (h_{DNA}) and molecular diameter of DNA molecules (ϕ_{DNA}) for DNA duplexes and mismatched DNA duplexes are shown as the "mean value \pm standard deviation". These values were calculated from one hundred data points derived from the STM images for each of the sample substrates.

Supporting Information Results

***In situ* STM measurements for single-stranded probe DNA immobilized substrates and random MM DNA duplexes substrates.**

Single-stranded DNA probes were immobilized on gold substrates, and investigated by *in situ* STM (**Figure 1 b**). The DNA duplex molecules were imaged as bright dots. Single-stranded DNA probes were closed-packed on the substrate surface. The average diameter for single-stranded probe DNA molecules is 1.0 ± 0.5 nm. This result indicates that the molecular images for single-stranded DNA are quite different from those for DNA duplexes (**Figure 1a**). When using random target DNA for hybridization, the DNA molecules were imaged as bright dots similar to that of single-stranded DNA molecules (data not shown). This result indicates that the random target DNA molecules could not hybridize with the probe DNA.

Cyclic voltammetry for gold substrates before and after immobilization of thiolated probe DNA.

To confirm the immobilization of thiolated probe DNA on the gold substrate for STM imaging, we investigated the substrate with electrochemical method (**ref. 10**). Prior to the cyclic voltammetry (CV) measurements, the gold electrodes are immersed in the probe DNA solution, as same as the gold substrates used for STM imaging. **Figure S1** shows a typical of the cyclic voltammogram for redox marker, ferricyanide (3-/4-), at the gold electrodes before and after immobilizations of probe-DNA. This result shows that the reduction and oxidation of ferricyanide is less reversible at probe DNA immobilized gold substrates, than at gold substrates. The irreversibility of the ferricyanide redox reaction was also observed for the substrates that used for STM measurements (data not shown). This is due to repulsive electrostatic interactions impeding the ability of the anions, ferricyanide ions, to reach the DNA-immobilized surface. Moreover, we prepared the various amount of the probe DNA immobilized on the gold electrodes by using the immersion of thiolated probe DNA solution containing the various salt concentrations. The CV measurements of ferricyanide redox reaction for large amount of probe DNA immobilized electrode (immersion of DNA solution containing 1M NaCl) were more irreversible than that for small amount of probe DNA immobilized electrode (immersion of DNA solution containing 1 mM NaCl). Therefore, these results confirmed that thiolated probe DNA molecules were immobilized on the gold substrate.

Cyclic voltammetry for probe DNA immobilized gold substrate before and after hybridization of target DNA.

To confirm the hybridization of target DNA with its probe DNA on the gold substrate used for STM measurements, we investigated the 2,6-disulfonic acid anthraquinone (AQDS) reaction on the DNA duplex immobilized gold substrate used for STM imaging (**ref.11**) by using cyclic voltammetry. It is well-known that the AQDS molecules do not bind single-stranded DNA, but selectively intercalated into DNA duplex. Therefore, the reaction peaks could confirm the hybridization of target DNA on the probe DNA immobilized substrates. Upon incubation of the sample substrates in 2,6-disulfonic acid

anthraquinone (AQDS) solution, a typical voltammetry peaks, consistent with the oxidation and reduction of AQDS, were observed (**Figure S2**). On the other hand, no voltammetric peak of AQDS was observed for single-stranded probe DNA modified gold substrates, and was also observed when the probe DNA modified surface was exposed to non-complementary target DNA.

5

SPR measurements for single-stranded or DNA duplexes immobilized on gold substrates.

To estimate the hybridization efficiency of target DNA molecules, relative to the complementary target DNA (PM DNA), we investigate the probe-DNA immobilized gold substrates by using surface plasmon resonance spectroscopy (Biocore T100). From the increase of the SPR response after exposure of target DNA, we estimated the amount of the hybridized target DNA molecules on the probe DNA immobilized substrates, and then calculated the hybridization efficiency for middle 1MM DNA, middle 2MM, random MM, and terminal 1MM, relative to PM DNA (**Table S1**). This result shows that the increase in mismatched base in the target DNA sequence resulted in the decrease of the hybridization efficiency of target DNA, relative to the PM DNA, which is comparable to the values that were calculated from our STM imaging results. However, the observed hybridization efficiency calculated by STM was found to be smaller than that were calculated by SPR results. Since those STM images reflect the electronic wavefunctions for the DNA duplex and single-strand DNA on the surface, this difference might be due to the poor electronic contact with gold substrate induced by a mismatch base pair, resulting in the decrease of the observed number of the DNA duplex in the STM images.

20

Denaturing of DNA duplexes on the surface substrate.

DNA duplexes in the substrate surface were denatured thermally. Upon heating of the substrate in the buffer solution, the DNA duplexes were denatured, resulting in a decrease of the number of DNA duplexes in the STM image. **Figures S3a-c** show the denaturing behavior of DNA duplex substrates. The decrease in the number of DNA duplex images started at 45°C (**Figure S3 b**) and was completed at

25

60°C (**Figure S3 c**). This result indicates that DNA duplexes on the surface were denatured by heating. In addition, DNA duplexes on the surface were less stable than in bulk solution, in which the melting temperature for the target DNA was 58°C. This difference might be due to charge repulsion induced by closer packing of anionic DNA duplexes in this situation, relative to bulk solution. The denatured probe DNA molecules were rehybridized with target DNA (**Figure S3 d**). Upon immersion of the denatured probe DNA *in the random DNA solution*, we observed no DNA duplex molecular images on the substrate, but only probe single-stranded DNA images (**Figure S3e**), similar to the results (**Figure 1b**). Therefore, this result indicates that the denatured probe DNA molecules were not hybridized with random target DNA.

10

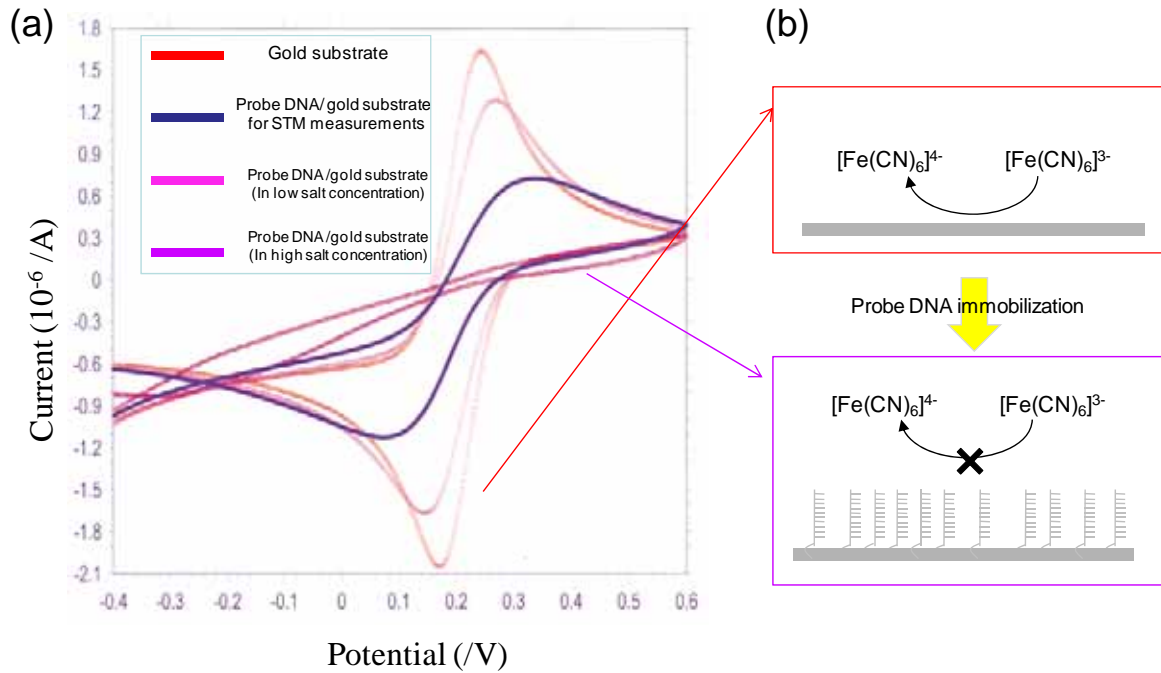
Optimization of the hybridization solutions for single-molecule STM imaging of DNA duplexes

In this study, we successfully achieved the single-molecule STM imaging of DNA duplexes. This should be due to the optimal solution condition, especially optimal divalent cation (Mg^{2+}) concentration for DNA-hybridization. Note that, in order to increase the efficiency for immobilization of probe DNA and hybridizations of target DNA with the probe DNA, the divalent cations, *e.g.*, Mg^{2+} , have been required and commonly been used for the immobilization and hybridization process because the cations prevent the intermolecular repulsion of the phosphate backbones of DNA duplexes (**ref. S1**). In fact, upon hybridization in without or low Mg^{2+} concentration solution (0-1 mM) (*e.g.*, 0 mM: **Figure S3a**, 1 mM: **Figure S3b**), the hybridization efficiency for the DNA duplexes was significantly lower in these conditions, relative to in the situation in **Figure 1a** (12.5 mM). This confirmed that the proper concentration of the divalent cations is necessary for high efficiency hybridizations on the surfaces. On the other hand, an excess concentration of the divalent cations should induce intermolecular aggregation of DNA duplexes, resulting in preventing single-molecule imaging of DNA duplexes (**ref. S2**). Upon hybridizations performed in high Mg^{2+} concentration (50-200 mM) (*e.g.*, 100 mM: **Figure S3c**), we also found that the DNA duplex molecules are imaged as the clusters and/or aggregates of DNA duplexes, which is identical to the images of DNA duplex clusters reported previously (**ref.7,8,9,10**). Therefore,

we concluded that, for this hybridization process, the optimal concentration of Mg^{2+} is important in order to obtain single-molecule STM images of DNA duplexes, and determined that the optimal concentration of Mg^{2+} for the hybridization solution is in the range of 10-20 mM for single-molecule STM imaging, without the DNA coagulations and poor hybridization.

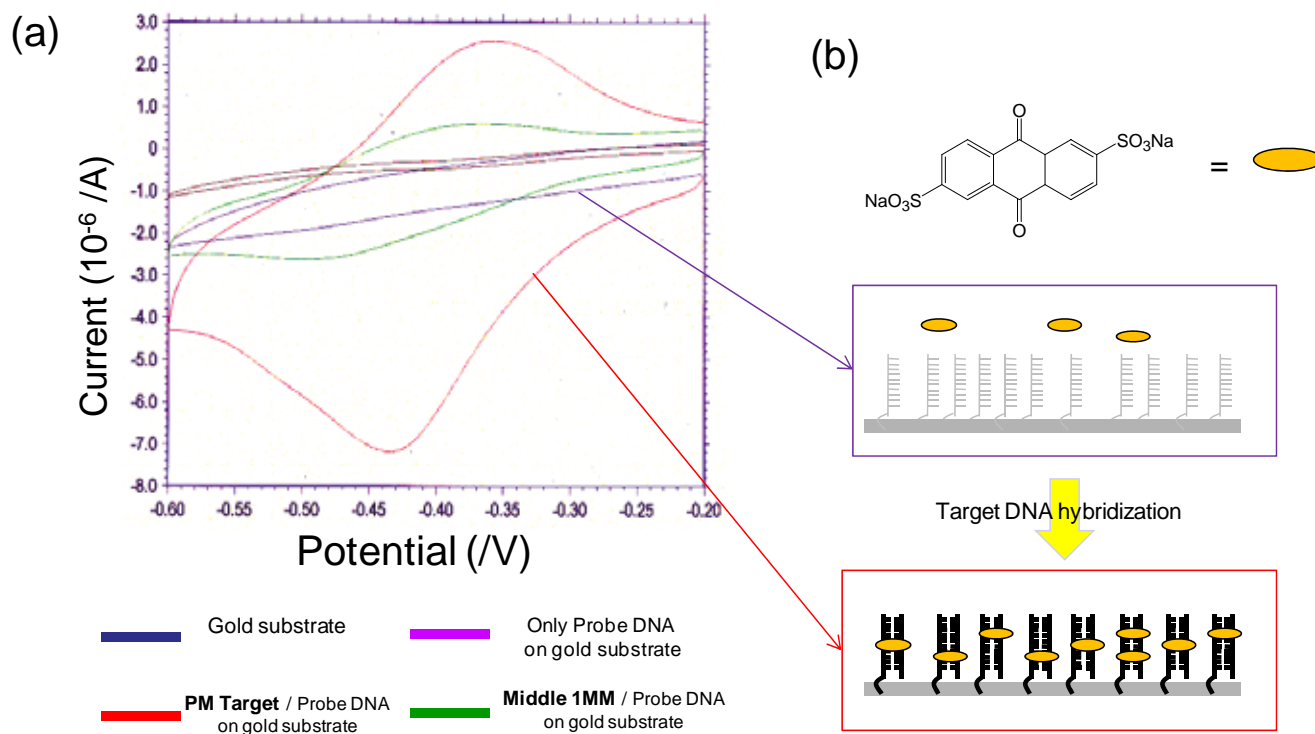
Supporting Figure and Figure captions

Figure S1 and its Captions Cyclic Voltammogram before and after the immobilization of probe DNA on the gold substrate.



- 5 (a) Cyclic voltammogram of a gold electrode (red) prior to immobilization of probe DNA, and after immobilization of probe-DNA in 50 mM phosphate buffer containing 12.5 mM MgCl_2 solution, as same as that used for STM sample substrates (blue), in 1 mM NaCl solution (pink), and in 1 M NaCl solution (purple). The scan rate was 100 mVs^{-1} . This peak shift of the ferricyanide ($[\text{Fe}(\text{CN})_6]^{4-/3-}$) redox-reaction at the probe DNA immobilized electrode (blue, purple and pink) is
- 10 due to repulsive electrostatic interactions impeding the ability of the anions, ferricyanide ions, to reach the DNA-immobilized surface. Therefore, these results confirmed that thiolated probe DNA molecules were immobilized on the gold substrate.
- (b) Schematics of redox reaction of ferricyanide (3-/4-) on gold electrode (upper figure), and probe-DNA immobilized gold substrate (lower figure).

Figure S2 and its Legends: Cyclic Voltammogram before and after the hybridization of target DNA with probe DNA on the gold substrate.

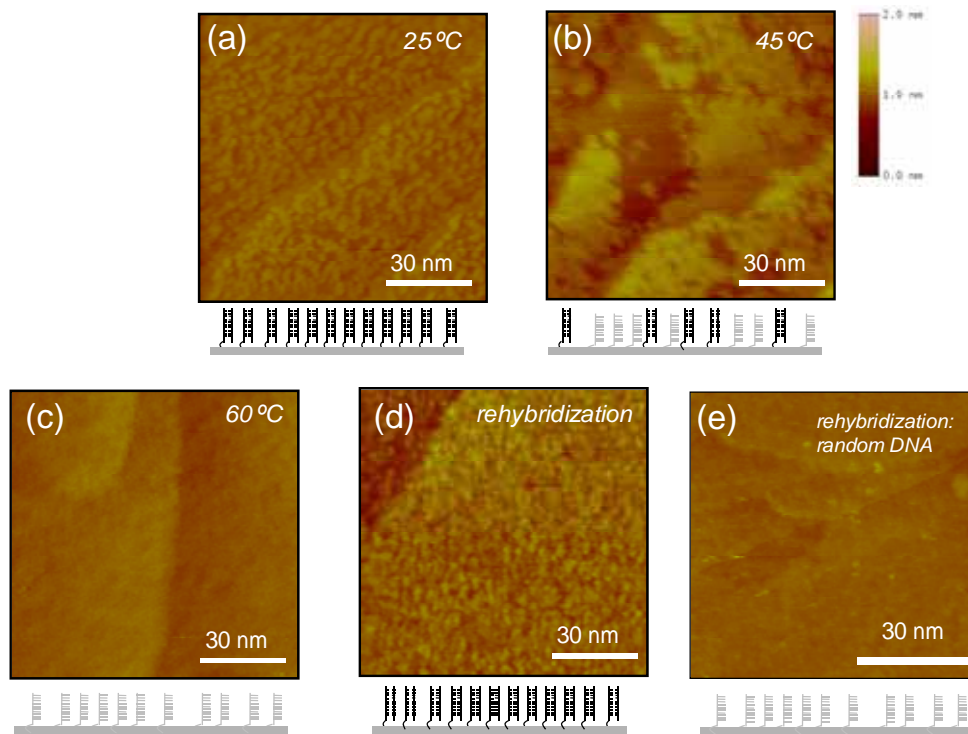


5

(a) Cyclic voltammogram of an gold electrode before immobilization of probe DNA (blue), after immobilization of probe DNA (purple), after hybridization of perfect-matched DNA (PM target DNA), as same as that used for STM sample substrates (red), and after hybridization of single base mismatched DNA (Middle 1MM target DNA) (green). To record these CVs, the electrodes was incubated in the 1mM AQDS solution overnight and then rinsed in phosphate buffer and place in an AQDS-free 0.05M phosphate buffer (pH 7.0) solution at a scan rate of 100 mVs^{-1} . This presence of the AQDS reaction peaks (red, green) confirmed the hybridization of target DNA on the probe DNA immobilized substrates. This is because AQDS molecules selectively intercalated into DNA duplex.

15 (b) Schematics of redox reaction of intercalated AQDS molecules on gold electrode before (upper figure) and after hybridization of target DNA with the probe DNA on the gold substrate (lower figure).

Figure S3 and its Legends: Hybridization and rehybridization by thermal cycles.

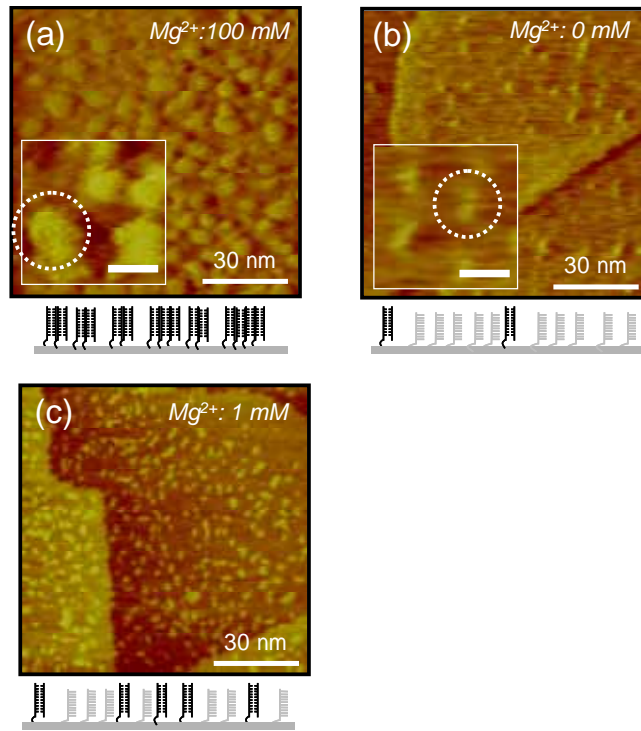


5 STM images ($100 \text{ nm} \times 100 \text{ nm}^2$) of perfectly matched DNA duplexes immobilized on gold substrates
(a) before dehybridization, (b) after dehybridization at 45°C for 30 min, (c) 60°C for 30 min, and (d)
after rehybridization. The sample substrate used for this data is the same for these figures.

10

15

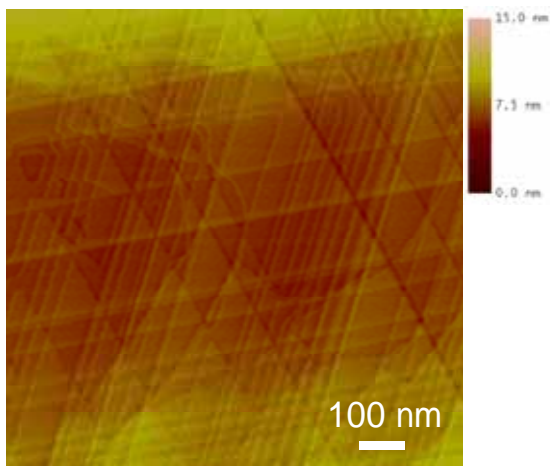
Figure S4 a-c and its Legends:



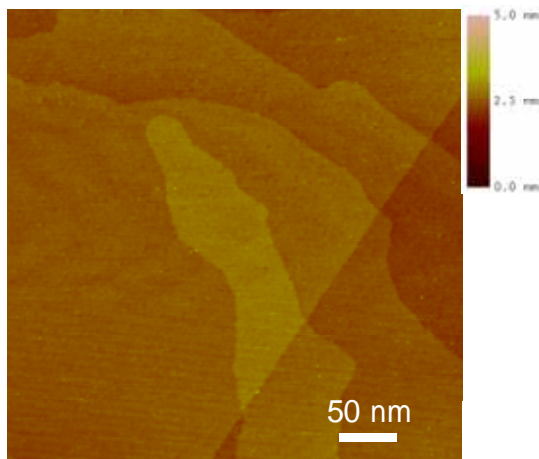
5 STM images ($100 \text{ nm} \times 100 \text{ nm}^2$) of perfectly-matched DNA duplexes immobilized on a gold substrate following hybridization in phosphate buffer solution containing Mg^{2+} concentrations of (a) 100 mM, (b) 0 mM and (c) 1 mM. The magnified image ($15 \text{ nm} \times 15 \text{ nm}^2$) for coaggregated DNA duplexes (a) and single-molecule duplexes (b-c), and are shown in the inset. The substrate potential (E_{sub}) was -200 mV, and the bias voltage (E_{bias}) was +200 mV (sample negative). The tunneling current (I) was 200 pA.

Figure S4 d,e and its Legends:

(c)







(e)



(d) STM images ($1000 \text{ nm} \times 1000 \text{ nm}^2$) of gold substrates (e) The magnified image ($400 \text{ nm} \times 400 \text{ nm}^2$) is shown. The substrate potential (E_{sub}) was -200 mV , and the bias voltage (E_{bias}) was $+200 \text{ mV}$ (sample negative). The tunneling current (I) was 200 pA .

Table S1:

Target DNA	$M_{density}$ ($\times 10^{12}$ probes/cm ²): Molecular Density	Target DNA Density Relative to PM DNA Density (STM)	Relative SPR signal of target DNA to PM DNA
 PM	6.53 \pm 0.40	-	-
 Middle 1MM	1.91 \pm 0.18	29.2%	43.6 %
 Middle 2MM	0.07 \pm 0.05	1.1 %	5.1 %
 Random MM	Not observed	0 %	1.5 %

The observed molecular density ($M_{density}$), and the target DNA density relative to perfect-matched DNA density (purple), and SPR signal intensity of target DNA relative to that for perfect-matched DNA (red). We used surface plasmon resonance spectroscopy to estimate the hybridization efficiency of mismatched target DNA molecules, relative to the complementary target DNA (PM DNA). The increase of the SPR response after exposure of target DNA was the amount of the hybridized target DNA molecules on the probe DNA immobilized substrates. The hybridization efficiency for middle 1MM DNA, middle 2MM, and random MM relative to PM DNA, were calculated by dividing the amount of PM DNA. Both of the STM and SPR results shows that the increase in mismatched base in the target DNA sequence resulted in the decrease of the hybridization efficiency of target DNA, relative to the PM DNA.

Supporting References

[S1] a) Ott, G.S.; Ziegler, R.; Bauer, W. R. *Biochemistry*, **1975**, 14, 3431-3438; b) Owczarzy, R.; Moreira, B. G.; You, Y.; Behlke, M. A.; Walder, J.A., *Biochemistry*, **2008**, 47, 5336-5353.

[S2] a) Duguid, J.; Bloomfield, V. A.; Benevides, J. M.; Thomas, G. J., Jr. *Biophys. J.*, **1995**, 69, 2623-2641; b) Kornyshev, A. A.; Leikin, S. *Proc. Natl. Acad. Sci. USA* **1998**, 95,13579-13584; c) Burak, Y.; Ariel, G.; Andelman, D. *Biophys. J.*, **2003**, 85, 2100-2110; d) Ceres, D. M.; Udit, A. K.; Hill, H.D.; Hill, M.G.; Barton, J. K. *J. Phys. Chem. B.*, **2007**,111,663-668.